



# Porphyrins Anchored onto Colour Catcher®: Photoactive Material for the Conversion of Amines into Imines and Aldehydes into Carboxylic Acids

Caterina Damiano,<sup>[a]</sup> Matteo Cavalleri,<sup>[a]</sup> Corrado di Natale,<sup>[b]</sup> Roberto Paolesse,<sup>[c]</sup> and Emma Gallo<sup>\*[a]</sup>

A new photoactive material was obtained by the heterogenization of zinc(II) porphyrin onto cellulose-based Colour Catcher® sheet. The so-obtained Zn(porphyrin)@CC material performed very well in activating molecular oxygen in the photooxidative coupling of amines to imines and the photooxidation of aldehydes to corresponding acids in the presence of white light.

The high eco-compatibility of the solid support, the chemical stability of the photoactive material and the mild experimental conditions applied confer a very good sustainability to the procedure and open the doors to a larger employment of Colour Catcher®-based porphyrin material in reactions mediated by light.

## Introduction

Light is the main source of energy for all living organisms and it is the greenest and most renewable resource on our planet. In the endless war against the global energy crisis,<sup>[1]</sup> which requires the development of efficient technologies for the fossil fuels-free conversion of energy, sunlight represents our best ally thanks to being inexpensive, abundant and inexhaustible. However, sunlight is not only a clean energy source<sup>[2-5]</sup> but also it is a precious tool to favor chemical transformations. Thinking about Nature, sunlight can be considered one of the catalysts of life in view of its crucial role in the activation of essential chemical processes, such as photosynthesis.<sup>[6]</sup>

Taking into account this natural model, many scientific efforts have been devoted in developing photochemical processes capable to exploit light to promote greener chemical transformations<sup>[7-9]</sup> by using homogenous and heterogeneous photocatalytic systems. The latter, which include both molecular catalysts and semi-conductive materials, have been widely

exploited in medicine,<sup>[10-13]</sup> environmental management,<sup>[14-16]</sup> and organic synthesis.<sup>[8,17-20]</sup>

The applications mentioned above are strictly related to the nature and the action mode of the employed photocatalysts, which can be classified as photoredox catalysts or photosensitizers (PSs). Photoredox catalysts, opportunely irradiated by light, exploit a *single electron transfer* (SET) mechanism that allows the exchange of electrons between the catalyst and the substrate through oxidative or reductive processes. Conversely, photosensitizers act by an *energy transfer* (ET) mechanism in which, after the irradiation, the excited state of the PS transfers the energy to a substrate (that cannot adsorb the light) making it reactive towards other reagents. Among all the developed photoredox catalysts and PSs, porphyrin macrocycles represent one of the most interesting classes of molecules that can be suitably modified to act both by SET or ET mechanism. In fact, thanks to their peculiar photophysical and electronic properties, porphyrin-based systems have been extensively employed as PSs in photodynamic therapy (PDT)<sup>[21-24]</sup> and photocatalysts in aerobic organic transformations.<sup>[25]</sup> In addition, the possibility to fine-tune the porphyrin properties by appropriate structural modifications makes them able to absorb light in all the UV-visible spectral range, including visible light.

For these reasons, scientific research is trying to further develop porphyrin-based photocatalytic systems especially to solve some typical drawbacks of photocatalysis, such as: i) the high cost and possible toxicity of the employed photocatalysts; ii) the low photocatalytic activity, particularly under visible or solar illumination and iii) the difficult handling and separation of the photocatalysts when employed under homogenous conditions.

To solve these issues, heterogenization strategies<sup>[26-28]</sup> could be a valuable solution through the anchoring, by covalent bonding or non-covalent interactions, active photocatalysts on suitable solid supports aiming to merge the high activity and selectivity of single-site catalysts with the easy recovery and recyclability of the heterogeneous ones. Several solid supports

[a] Dr. C. Damiano, M. Cavalleri, Prof. E. Gallo

Department of Chemistry

University of Milan

Via Golgi 19, 20133 Milan (Italy)

E-mail: emma.gallo@unimi.it

Homepage: <https://sites.unimi.it/emmagallogroup/>

[b] Prof. C. di Natale

Department of Electronic Engineering

University of Roma Tor Vergata

Viale del Politecnico, 00133 Rome (Italy)

[c] Prof. R. Paolesse

Department of Chemical Science and Technologies

University of Roma Tor Vergata

Via della Ricerca Scientifica 1, 00133 Rome (Italy)

Supporting information for this article is available on the WWW under <https://doi.org/10.1002/ceur.202300020>

© 2023 The Authors. ChemistryEurope published by Chemistry Europe and Wiley-VCH GmbH. This is an open access article under the terms of the Creative Commons Attribution License, which permits use, distribution and reproduction in any medium, provided the original work is properly cited.



have been tested for the heterogenization procedures and more importance has been given to naturally derived ones,<sup>[29]</sup> which, thanks to their abundance and low environmental impact, allow the development of cheaper heterogenized catalytic systems by preserving the intrinsic eco-compatibility of photocatalyzed reactions.

In this view, we recently reported the heterogenization of a porphyrin-based chemosensor for detecting mercury ions<sup>[30]</sup> on the commercially available Colour Catcher®, a naturally derived dye-trapping sheet commonly employed during the laundry to adsorb the colors released from clothing. The simple anchoring procedure of the active molecule and the high stability of the obtained heterogenized porphyrin makes the Colour Catcher® an attractive solid support also for anchoring porphyrin-based photocatalytic systems.

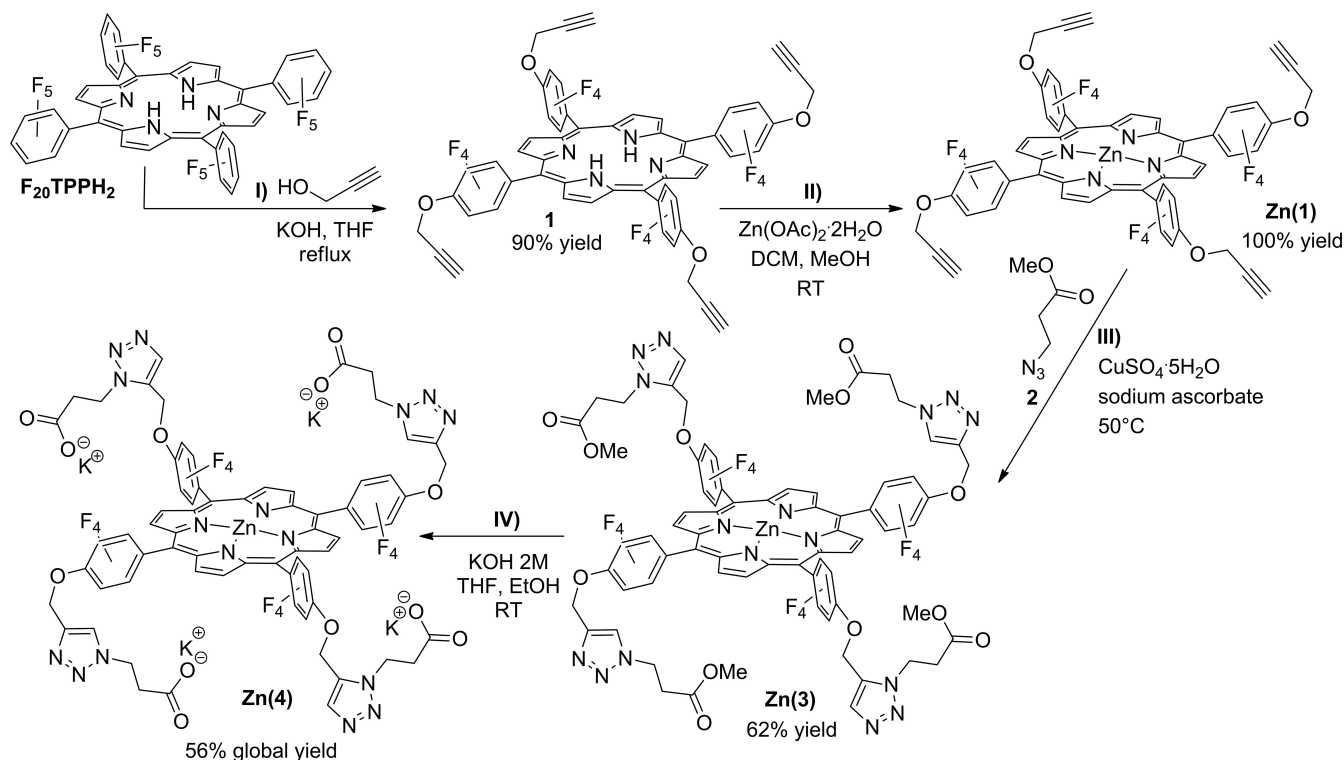
Thus, here we propose a low-cost heterogenized photoactive material, consisting of an opportunely functionalized zinc porphyrin bounded on Colour Catcher® sheet, which is capable of efficiently promoting the sustainable photooxidative coupling of amines and the photooxidation of aldehydes by activating molecular oxygen under white light.

## Results and Discussion

### Synthesis of the solid-supported Zn(4)@CC

Colour Catcher® sheets are made of ultra-absorbent naturally-derived fibres having positively charged groups on the surface

that during the wash electrostatically trap the negatively charged dyes released by tissues.<sup>[31]</sup> This action mode requires the introduction of anionic groups onto the porphyrin periphery to bind the macrocycle onto the Colour Catcher® surface by ionic interactions. In addition, the insertion of a central metal, such as zinc(II),<sup>[32,33]</sup> and the presence of halogen atoms<sup>[34]</sup> in the porphyrin structure can enhance the photocatalytic activity of porphyrin-based systems, especially to produce reactive oxygen species (ROSs).<sup>[35]</sup> Bearing in mind these assumptions, we synthesized a fluorinated zinc porphyrin, containing four negatively charged linkers, by following the multi-steps synthetic procedure shown in Scheme 1. As previously reported by us,<sup>[36]</sup> fluorinated aryl rings of *meso*-substituted porphyrins can be easily functionalized through the nucleophilic substitution in the *para* position of the pentafluorophenyl moiety. Thus, F<sub>20</sub>TPPH<sub>2</sub> (*meso*-tetrakis(pentafluorophenyl) porphyrin) was refluxed with propargyl alcohol, in presence of KOH, to achieve in 90% yield the desired *tetra*-substituted porphyrin **1** (step I, Scheme 1), which showed four terminal propargyl functionalities useful to perform an azide/alkyne cycloaddition (click reaction). To protect the porphyrin *core* from the undesired metalation by copper, whose salts are commonly employed to catalyze “click reactions”,<sup>[37]</sup> porphyrin **1** was firstly reacted with Zn(OAc)<sub>2</sub>·2H<sub>2</sub>O (step II, Scheme 1) affording the metalated Zn(**1**) in a quantitative yield. Then, the desired triazole spacers were introduced by reacting Zn(**1**) with methyl-3-azide-propionate (**2**), previously synthesized and purified, in the presence of CuSO<sub>4</sub>·5H<sub>2</sub>O and sodium ascorbate (step III, Scheme 1) that provided Zn(**3**) in 62% yield.

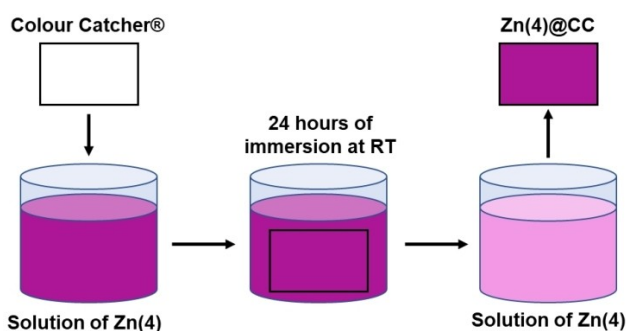


Scheme 1. Multi-steps synthetic procedure adopted to synthesize the negatively charged Zn(4).



The obtained **Zn(3)**, which shows four terminals –COOMe groups, was treated with KOH (2.0 M) to yield the anionic carboxylate moieties (Scheme 1, path IV) that are required for the porphyrin anchorage onto the Colour Catcher® sheet. The isolation of **Zn(4)** as a pure solid from the reaction mixture was hampered by the amphiphilic nature of **Zn(4)**, which was responsible for the formation of a jellylike mixture when either the reaction medium was evaporated to dryness or an apolar solvent was added to favor the precipitation of the desired compound. As a consequence, the recovered mixture containing **Zn(4)** was employed for the anchoring procedure without further purifications. Conversely, porphyrins **1**, **Zn(1)** and **Zn(3)** were easily isolated and fully characterized by <sup>1</sup>H, <sup>13</sup>C and <sup>19</sup>F NMR spectroscopies, UV-visible spectrophotometry, mass spectrometry and elemental analysis. Considering that acquired data (see experimental) indicated the quantitative conversion of **Zn(3)** into **Zn(4)**, the adopted multi-steps strategy allowed the synthesis of **Zn(4)** in 56% of global yield and without applying long and expensive purification procedures for all the steps reported in Scheme 1.

At this point, the **Zn(4)**-containing solution was employed to perform the simple heterogenization procedure reported in Scheme 2. According to the operating mechanism of Colour Catcher®, which exploits its function when it is dipped in a dye solution, the direct immersion of Colour Catcher® sheets into the **Zn(4)**-containing solution was adopted as the anchoring strategy. However, the amount of porphyrin loaded onto the solid support resulted strictly dependent on the porphyrin concentration and the immersion time. In order to ensure the anchorage reproducibility, 92 cm<sup>2</sup> of a Colour Catcher® sheet was dipped into 50.0 mL of **Zn(4)** solution, with a fixed concentration of 1.50 × 10<sup>-3</sup> M, for 24 h at room temperature in order to maximize the amount of **Zn(4)** bonded onto the solid surface. Then, the obtained **Zn(4)@CC** was dried and washed with distilled water, THF and CH<sub>3</sub>CN to remove the porphyrin excess and no substantial porphyrin leaching was observed during the various washing steps. The amount of **Zn(4)** loaded onto the solid support was calculated by UV-visible spectrophotometry by measuring the **Zn(4)** concentration before and after the immersion of the sheet and collected data allowed estimating an average value of anchored **Zn(4)** equal to 0.24 mg/cm<sup>2</sup>.



Scheme 2. Heterogenization procedure employed to obtain **Zn(4)@CC**.

To verify the success of the heterogenization and the porphyrin distribution onto the sheet, the obtained **Zn(4)@CC** was characterized by UV-visible spectrophotometry, Scanning Electron Microscopy (SEM) and Energy Dispersive X-Ray Analysis (EDX). In view of the sensibility of each technique and the spectroscopic properties of zinc porphyrins, three different samples of **Zn(4)@CC** were prepared in order to achieve three distinct loadings of **Zn(4)** on the solid surface (0.04 mg/cm<sup>2</sup>, 0.17 mg/cm<sup>2</sup> and 0.24 mg/cm<sup>2</sup>). Due to the high adsorption of porphyrins in the UV-visible spectral range, only the most diluted sample (**Zn(4)@CC** 0.04 mg/cm<sup>2</sup>) resulted suitable for the UV-visible characterization. As reported in Figure 1a, the solid-supported **Zn(4)@CC** preserved the typical spectral profile of zinc porphyrins in solution by showing a distinguishing adsorption band at 428 nm (Soret band) and one well resolved Q band at 553 nm.

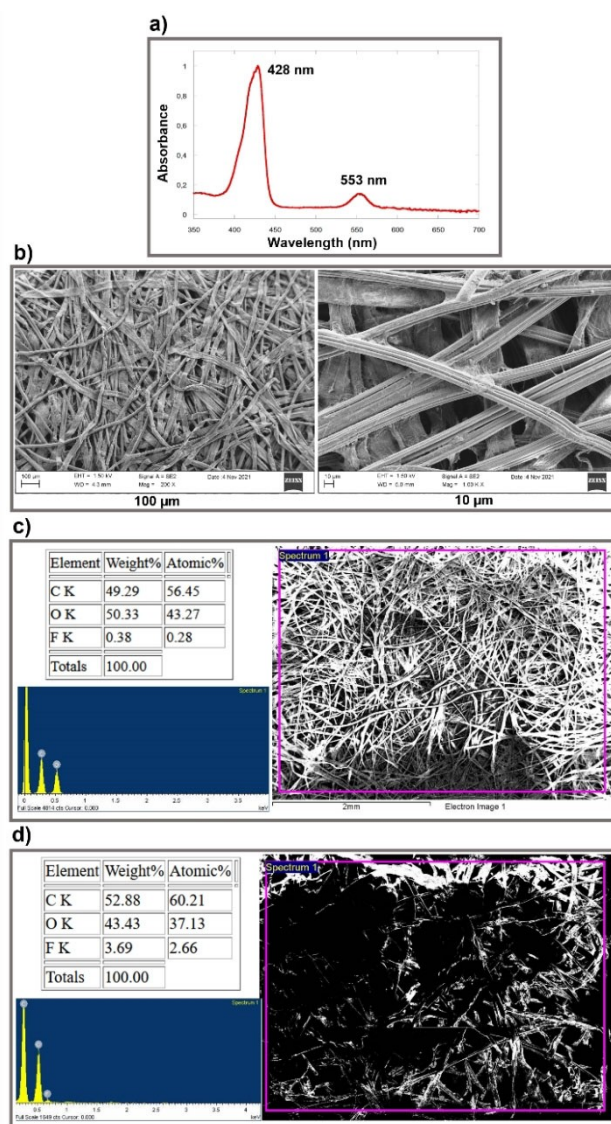


Figure 1. Characterization of **Zn(4)@CC**: a) UV-visible spectrum of **Zn(4)@CC** 0.04 mg/cm<sup>2</sup>, b) SEM images of **Zn(4)@CC** 0.17 mg/cm<sup>2</sup>; c) EDX analysis of **Zn(4)@CC** 0.17 mg/cm<sup>2</sup> and d) EDX analysis of **Zn(4)@CC** 0.24 mg/cm<sup>2</sup>.



According to our previous characterization of anionic porphyrins anchored on the Colour Catcher® surface,<sup>[30]</sup> both adsorption bands of Zn(4)@CC were slightly red-shifted than those observed for the Zn(4) porphyrin in solution, placed at 420 nm (Soret band) and 551 nm. These red-shifts, together with the sharp profile of the Soret band of Zn(4)@CC, suggested the absence of porphyrin aggregation onto the solid surface. In addition, the dense and homogenous texture of Zn(4)@CC was confirmed by SEM images (Figure 1b), acquired for the Zn(4)@CC 0.17 mg/cm<sup>2</sup> sample, which highlighted the applicability of Colour Catcher® as platform for the uniform heterogenization of negatively charged porphyrin species.

Finally, the chemical composition of Zn(4)@CC was achieved by performing EDX analysis on the two more concentrated samples, 0.17 mg/cm<sup>2</sup> and 0.24 mg/cm<sup>2</sup>, whose data are reported in Figures 1c and 1d, respectively.

Both EDX spectra revealed oxygen, carbon, and fluorine as major elements on the solid surface according to the co-presence of cellulose-based fibers and fluorinated porphyrins. Comparing the two EDX analyses, the increasing percentages of fluorine and carbon and the simultaneous decrease of oxygen, observable in Figure 1d, confirmed the greater loading of zinc porphyrin for unit of solid surface in the most concentrated sample (Zn(4)@CC 0.24 mg/cm<sup>2</sup>).

The homogenous distribution of Zn(4) onto the Colour Catcher® surface demonstrated the applicability of these cellulose-based sheets as suitable supports for the heterogenization of homogenous species. In addition, the high availability and the low-cost of this commercially available product make its use in chemical fields an interesting approach to respond to the increasing demand for economic, easy to handle and recyclable systems.

### Photooxidative coupling of amines promoted by Zn(4)@CC

In view of the well-known ability of porphyrin-based systems to act as photocatalysts or photosensitizers, Zn(4)@CC was tested as photoactive material in the conversion of amines into imines. To combine the low-cost of the heterogenized Zn(4)@CC with an energy saving, simple and reproducible process, we pointed out our studies on the use of low consumption and easily available light sources, such as the commercially available LED strips that can be simply found in common electronics stores.

By employing 600 lumen white LEDs that simulate the natural light (color temperature: 4000 K), we found that Zn(4)@CC can behave as an efficient photoactive material able to promote the photooxidative coupling of amines under very mild conditions.

Bearing in mind that the photooxidation of organic substrates can take place through the formation of singlet oxygen (<sup>1</sup>O<sub>2</sub>), the main ROS produced by porphyrin-based photosensitizers, the study of the photooxidative coupling of amines promoted by Zn(4)@CC was performed by employing acetonitrile (CH<sub>3</sub>CN) as the solvent in order to ensure a longer singlet oxygen lifetime.<sup>[38]</sup> At this point, the role of the reaction parameters (catalytic loading, reaction temperature and reac-

tion time) was evaluated by using benzyl amine as the model substrate (Table 1). In order to assess the role of Zn(4)@CC, the model reaction was first irradiated in absence of photoactive species for 4 or 6 h at 50 °C under pure oxygen atmosphere (99.95 % O<sub>2</sub>) (entries 1–2, Table 1). Only traces of the desired imine **5** were detected. Conversely, the addition of the sole 0.3 % mol of Zn(4)@CC under the same experimental conditions was responsible for the formation of **5** in 68 % and 98 % yields (entries 3–4, Table 1) after 4 and 6 h of irradiation, respectively. It should be noted that the desired product **5** was obtained in a quantitative yield also at room temperature (entry 5, Table 1) after 6 h of irradiation. The decrease of the catalytic loading from 0.3 % to 0.15 % mol provoked the slight decrease of the reaction yield to 85 % (entry 7, Table 1). The influence of the oxygen concentration was also evaluated and the model reaction was performed under air (~21 % O<sub>2</sub>), both at room temperature and 50 °C. Unfortunately, the aerobic photooxidative coupling yielded the desired imine **5** in lower yields (entries 8–10, Table 1) with respect to those obtained under oxygen atmosphere suggesting the importance of the oxygen concentration in the production of ROSs. The above-described optimization of the procedure highlighted that the photooxidative coupling of amines can be efficiently carried out in the presence of 0.3 % mol of Zn(4)@CC by irradiating the reaction mixture with white LEDs for 6 h at room temperature under oxygen atmosphere. Even if 0.15 % mol of Zn(4)@CC showed good performances in the synthesis of **5**, the subsequent study was performed by using 0.3 % mol of Zn(4)@CC in order to maximize the reaction productivity. The use of a more concentrated heterogeneous catalyst is not a drawback due to the good recyclability of the photoactive material, which can be reused at least three consecutive times without any loss of activity. The recycling test revealed a very good chemical stability of the catalytic material. In fact, the desired compound was formed in 99 % yield in the first and second run and in 98 % yield in the third one. Recorded data excluded degradation processes of the photocatalyst during the oxidation reaction.

**Table 1.** Optimization of the reaction conditions for the photooxidative coupling of benzyl amine by using Zn(4)@CC as photoactive material.<sup>[a]</sup>

Entry	Zn(4)@CC loading [% mol]	Atmosphere	T [°C]	t [h]	Yield <sup>[b]</sup> [%]
1	–	O <sub>2</sub>	50	4	–
2	–	O <sub>2</sub>	50	6	traces
3	0.3	O <sub>2</sub>	50	4	68
4	0.3	O <sub>2</sub>	50	6	98
5	0.3	O <sub>2</sub>	RT	6	100
6	0.15	O <sub>2</sub>	50	6	99
7	0.15	O <sub>2</sub>	RT	6	85
8	0.3	Air	50	6	30
9	0.3	Air	RT	6	19
10	0.15	Air	50	6	20

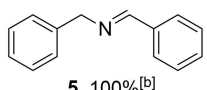
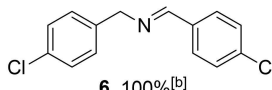
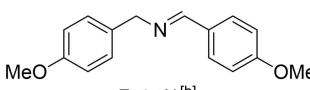
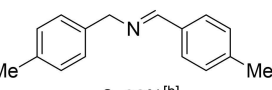
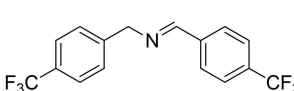
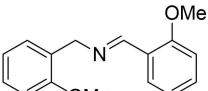
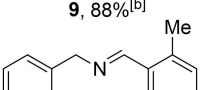
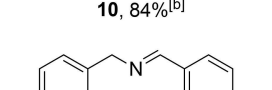
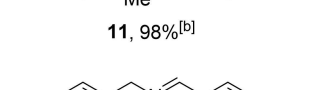
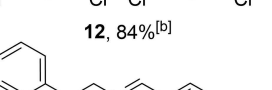
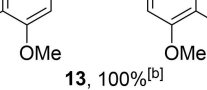
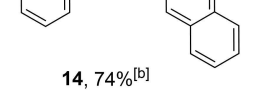
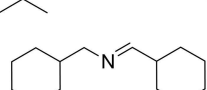
[a] Reactions were performed by irradiating with a white LED strip and by varying the Zn(4)@CC loading, temperature, oxygen concentration and reaction time. [b] Determined by <sup>1</sup>H NMR using mesitylene as the internal standard and calculated on the half of the initial amine moles.





To prove the general applicability of **Zn(4)@CC** as photoactive material, the photooxidative coupling of a series of amines was performed under the established optimized reaction conditions (Table 2). All the tested amines were efficiently converted into desired imines in yields up to 100%. As reported in Table 2, the presence of EWGs (electron-withdrawing groups) or EDGs (electron-donating groups) in the *para* position of the aromatic ring did not affect the reaction productivity and products **5–9** were obtained in comparable yields. Even the presence of EWGs or EDGs in *ortho* or *meta* positions did not influence the reaction performance and products **10–13** were formed in excellent amounts. On the other hand, the lower yield (74%) of product **14** can be ascribed to the steric hindrance of the naphthalene group. Unfortunately, no products were detected by replacing benzyl amine analogous with other primary amines, such as *n*-butyl, *iso*-propyl amine and cyclohexanemethylamine as well as aromatic amines such as aniline.

According to published data,<sup>[39–41]</sup> the photooxidative coupling of amines can occur through different reaction pathways, which depend on the nature of the generated ROS. As reported in

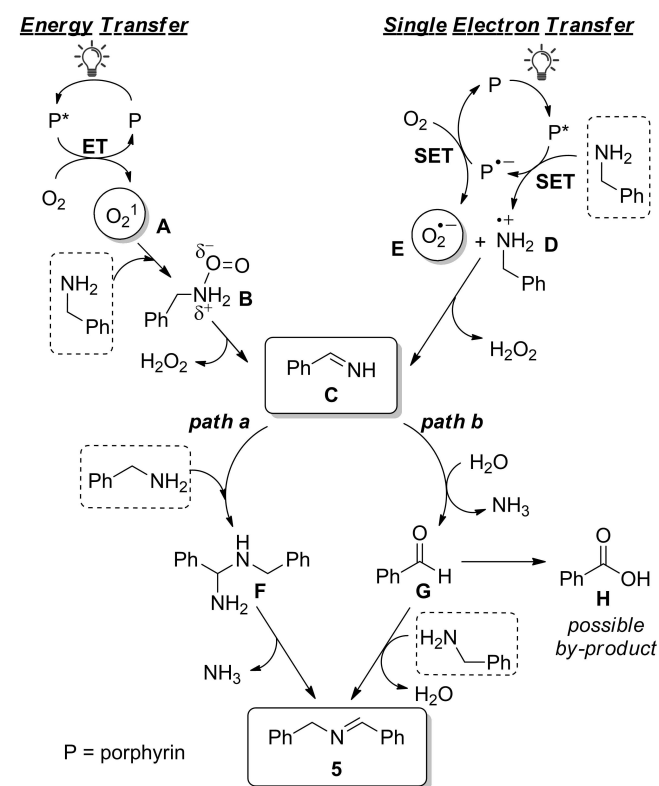
Table 2. Photooxidative coupling of amines promoted by <b>Zn(4)@CC</b> as photoactive material. <sup>[a]</sup>	
$2 \text{ R-NH}_2 \xrightarrow[\text{O}_2, \text{ white LED, RT, CH}_3\text{CN}]{\text{Zn(4)@CC}} \text{ R-N=CH-R} + \text{NH}_3 + \text{H}_2\text{O}_2$	
	
<b>5</b> , 100% <sup>[b]</sup>	<b>6</b> , 100% <sup>[b]</sup>
	
<b>7</b> , 94% <sup>[b]</sup>	<b>8</b> , 92% <sup>[b]</sup>
	
<b>9</b> , 88% <sup>[b]</sup>	<b>10</b> , 84% <sup>[b]</sup>
	
<b>11</b> , 98% <sup>[b]</sup>	<b>12</b> , 84% <sup>[b]</sup>
	
<b>13</b> , 100% <sup>[b]</sup>	<b>14</b> , 74% <sup>[b]</sup>
	
<b>15</b> , n.d. <sup>[b]</sup>	<b>16</b> , n.d. <sup>[b]</sup>
	
<b>17</b> , n.d. <sup>[b]</sup>	

[a] Reactions were performed at room temperature, under oxygen atmosphere for 6 h by irradiating with a white LED and using 0.3% mol of **Zn(4)@CC**. [b] Determined by <sup>1</sup>H NMR using mesitylene as the internal standard and calculated on a half of the initial amine moles.

Scheme 3, singlet oxygen and superoxide radical anion can be formed by an energy transfer (ET) or a single electron transfer (SET) mechanism, respectively. When the ET mechanism takes place, the excited porphyrin (**P\***), obtained after light irradiation, releases its energy to molecular oxygen to produce singlet oxygen (**A**). The latter can react with amine to form intermediate **B** that evolves to key-imine **C** releasing hydrogen peroxide as the by-product. Imine **C** can be also formed by a SET mechanism in which **P\*** abstracts one electron from the starting amine forming the radical cation **D** and the porphyrin radical anion (**P<sup>-</sup>**), which transfers its additional electron to molecular oxygen to produce the superoxide radical anion **E**. The direct reaction of **D** with **E** affords the intermediate imine **C**.

At this point, imine **C** can evolve into the final product following two different reaction pathways. In the first one, imine **C** can undergo a nucleophilic attack by the amine forming intermediate **F** that produces the desired imine **5** after ammonia elimination (*path a*, Scheme 3). On the other hand, imine **C** can be hydrolyzed by water traces yielding its corresponding aldehyde **G** (whose side-oxidation can form the corresponding acid **H**) that directly reacts with the starting amine to form product **5** and water (*path b*, Scheme 3).

In view of these mechanistic proposals, we firstly investigated the nature of the involved ROS by performing the synthesis of **5** in the presence of either 1,4-diazabicyclo[2.2.2]octane (DABCO) or benzoquinone (BQ), which are efficient trapping agents<sup>[42]</sup> for singlet oxygen and superoxide radical anion, respectively. Obtained data revealed that



Scheme 3. Possible reaction pathways for the photooxidative coupling of benzyl amine.



the quantitative yield of **5**, achieved after 6 h of irradiation in the presence of the sole **Zn(4)@CC** (entry 1, Table 3), dropped to 16% and 43% when either 5% mol of DABCO (entry 2, Table 3) or BQ (entry 3, Table 3) was present in the reaction medium. These data suggested that the photoactive **Zn(4)@CC** could form reactive oxygen species through both ET and SET mechanisms that can be both responsible for the photooxidative coupling of amines.

As reported in Scheme 3, two possible pathways can occur to convert imine **C** into the desired compound **5**. Thus, we tried to detect the formation of intermediate aldehyde **G**, or the corresponding carboxylic acid **H** that can be obtained by ROS oxidation (*path b*, Scheme 3). Considering the possible positive role of traces of water in the formation of aldehyde, the synthesis of **5** was performed either in the sole acetonitrile or in CH<sub>3</sub>CN/H<sub>2</sub>O (8:2) mixture and the reaction was monitored by IR spectroscopy. In both cases, neither benzaldehyde **G** nor benzoic acid **H** was detected and the desired imine **5** was formed in comparable yields (entries 4–5, Table 3). Obtained data suggest that either compounds **G** and **H** are not formed during the reaction or the coupling of benzyl amine with benzaldehyde is faster than its photooxidation to benzoic acid **H** and consequently the accumulation (and detection) of benzaldehyde **G** was avoided.

Thus, the **Zn(4)@CC**-promoted synthesis of **5** was repeated by introducing a stoichiometric amount (with respect to starting benzylamine) of benzaldehyde from the beginning of the reaction in order to investigate the possible formation of benzoic acid **H** as a reaction side-product. As reported in Table 3, the desired imine **5** was obtained in a quantitative yield both at room temperature and at 50 °C (entries 6–7, Table 3), the complete benzaldehyde conversion was always observed, and no traces of benzoic acid were found although the temperature was increased to favor the aldehyde oxidation. These data confirmed that the reaction of aldehyde with benzyl amine affording **5** is preferred and even if the formation of aldehyde by *path b* cannot be excluded, its high reactivity

towards benzyl amine should avoid its detection and its photooxidation to corresponding acid **H**.

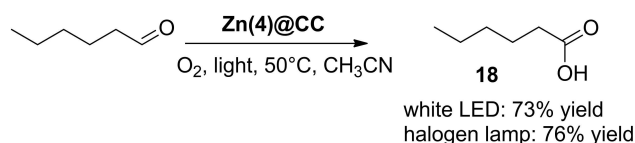
On the other hand, when the sole benzaldehyde was irradiated in the presence of **Zn(4)@CC** by applying experimental conditions reported in Table 3, the corresponding benzoic acid **H** was quantitatively achieved. Even if this last experiment did not shed some light to the most plausible mechanism of the imine formation, it proved the photoactivity of **Zn(4)@CC** also in the photooxidation of aldehydes.

Thus, we decided to better investigate this reaction that, alongside being a synthetic method for producing acids, can be considered a valuable method to establish the presence of aldehydes. These result assumes a relevance in view of the importance in developing analytical methods for aldehyde detection because these compounds (i.e. *n*-hexanal) can be considered markers of critical situations such us degradation of stored foods,<sup>[43]</sup> health hazards due to stored wood pellets<sup>[44,45]</sup> and medical diseases like pulmonary diseases and lung cancer.<sup>[46,47]</sup>

### Photooxidation of aldehydes promoted by **Zn(4)@CC**

The photoactive **Zn(4)@CC** was employed in the *n*-hexanal oxidation to hexanoic acid (**18**) (Scheme 4) by using experimental conditions reported in Table 3. Compound **18** was obtained in 65% yield and, when the temperature was increased from RT to 50 °C, a small increase of the reaction yield (73% yield) was achieved. The reaction productivity was slight better by replacing white LED with a 240 V halogen lamp (76% yield).

IR spectroscopy was employed to monitor the reaction outcome by following the growth of the C=O IR band of hexanoic acid at 1739 cm<sup>-1</sup>. The activity of heterogenized **Zn(4)@CC** material was compared to that of its homogenous precursors **Zn(F<sub>20</sub>TPP)**, **Zn(1)** and **Zn(3)** as well as that of the blank photooxidation of *n*-hexanal (performed in absence of any zinc porphyrin species). Due to the very low solubility of zinc porphyrins in acetonitrile, homogenous tests with **Zn(F<sub>20</sub>TPP)**, **Zn(1)** and **Zn(3)** porphyrins were carried out in CH<sub>3</sub>CN/CH<sub>2</sub>Cl<sub>2</sub> (9:1) mixture as the reaction solvent while the heterogeneous test in the presence of **Zn(4)@CC** was performed in pure CH<sub>3</sub>CN. All the reactions were carried out at 50 °C under oxygen atmosphere by irradiating with a 240 V halogen lamp in the presence of 0.3% mol of zinc porphyrin. The progress of the *n*-hexanal photooxidation was monitored by acquiring IR spectra at different reaction times (zero-time, 30 min, 1, 2 and 3 h) and considering the IR region between 1700 cm<sup>-1</sup> and 1800 cm<sup>-1</sup>, in which the two distinguish C=O stretching at 1722 cm<sup>-1</sup> and 1739 cm<sup>-1</sup> were attributed to *n*-hexanal and hexanoic acid (**18**), respectively. Thus, the intensity of the above-mentioned peaks



Scheme 4. Photooxidation of *n*-hexanal promoted by **Zn(4)@CC**.

Table 3. Photooxidative coupling of benzyl amine in presence of additives and by using **Zn(4)@CC** as photoactive material.<sup>[a]</sup>

Entry	Solvent	Additive	T [°C]	T [h]	Yield <sup>[b]</sup> [%]
1	CH <sub>3</sub> CN	–	RT	6	100
2	CH <sub>3</sub> CN	DABCO (5% mol)	RT	6	16
3	CH <sub>3</sub> CN	BQ (5% mol)	RT	6	43
4	CH <sub>3</sub> CN	–	RT	2	44
5	CH <sub>3</sub> CN/H <sub>2</sub> O (8:2)	–	RT	2	48
6	CH <sub>3</sub> CN	Benzaldehyde (1 eq.)	RT	6	100
7	CH <sub>3</sub> CN	Benzaldehyde (1 eq.)	50	6	100

[a] Reactions were performed under oxygen atmosphere by irradiating with a white LED and using 0.3% mol of **Zn(4)@CC**. [b] Determined by <sup>1</sup>H NMR using mesitylene as the internal standard and calculated on the half of the initial amine moles.



was reported in function of time (Figure 2) to appreciate both the *n*-hexanal conversion and the hexanoic acid formation. As reported in Figure 2a, while the *n*-hexanal conversion was faster in the absence of any photoactive species (blank reaction), the best reaction selectivity was registered in the presence of

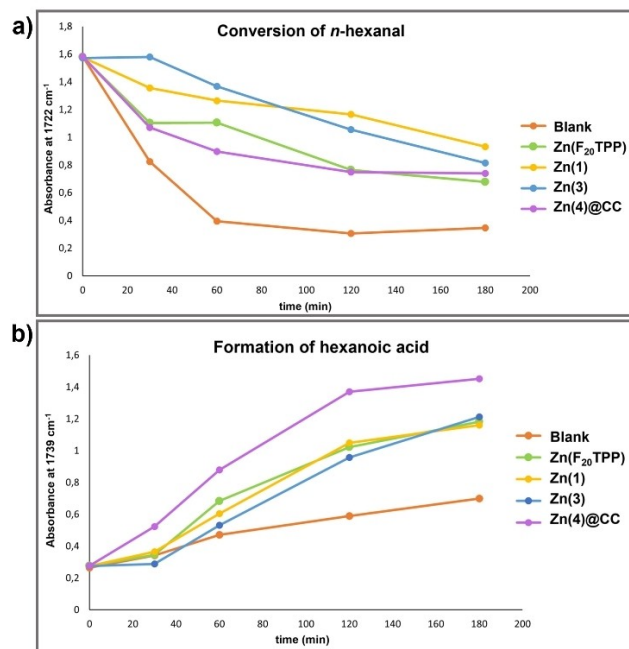


**Figure 2.** Comparison of the activity of Zn(F<sub>20</sub>TPP), Zn(1), Zn(3) and Zn(4)@CC in the photooxidation of *n*-hexanal: a) Conversion of *n*-hexanal in function of time and b) Formation of hexanoic acid (**18**) in function of time.

**Table 4.** Photooxidation of aldehydes promoted by Zn(4)@CC as photoactive material.<sup>[a]</sup>

$$\text{R-CHO} \xrightarrow[\text{CH}_3\text{CN, 50}^\circ\text{C, 6 hours}]{\text{Zn(4)@CC, O}_2, \text{halogen lamp}} \text{R-COOH}$$

<b>18</b> , 76% <sup>[b]</sup> (62% <sup>[c]</sup> ; 60% <sup>[d]</sup> )	<b>19</b> , n.d. <sup>[b]</sup>	<b>20</b> , 86% <sup>[b]</sup>	<b>21</b> , 85% <sup>[b]</sup>
<b>22</b> , 50% <sup>[b]</sup>	<b>23</b> , 100% <sup>[b]</sup>	<b>24</b> , 86% <sup>[b]</sup>	<b>25</b> , 65% <sup>[b]</sup>
<b>26</b> , 36% <sup>[b]</sup>	<b>27</b> , 30% <sup>[b]</sup>	<b>28</b> , 87% <sup>[b]</sup>	<b>29</b> , 76% <sup>[b]</sup>

[a] Reactions were performed at 50 °C, under oxygen atmosphere for 6 h by irradiating with a halogen lamp and using Zn(4)@CC 0.3% mol. [b] Determined by <sup>1</sup>H NMR using 2,4-dinitrotoluene as the internal standard. [c] The reaction was performed by using Zn(4)@CC 0.15% mol. [d] The reaction was performed by using Zn(4)@CC 0.075% mol.

Zn(4)@CC (Figure 2b). The blank reaction produced a smaller amount of **18** confirming that, in absence of appropriate photoactive systems, an unselective photooxidation can take place. On the contrary, the use of zinc porphyrins favored the synthesis of **18** as the major product under both homogenous and heterogeneous conditions. Comparable selectivities were observed by employing Zn(F<sub>20</sub>TPP), Zn(1) and Zn(3) suggesting that the introduction of functionalities with different lengths onto the *para* position of the pentafluorophenyl ring did not affect the productivity of the employed zinc porphyrin. To our delight, the best results were achieved by using the heterogenized Zn(4)@CC to underline that the heterogenization process had a positive effect on performances of the photoactive species.

In view of the good results achieved by using Zn(4)@CC in the *n*-hexanal photooxidation, we investigated the scope of the reaction by testing other aldehydes showing different electronic and steric properties (Table 4). Reactions were performed by applying experimental conditions described above (0.3% mol of Zn(4)@CC, 50 °C, oxygen atmosphere and CH<sub>3</sub>CN as the reaction solvent) and collected data indicated that Zn(4)@CC efficiently promoted the selective photooxidation of both alkyl and aryl aldehydes to corresponding carboxylic acids in yields up to 100% (Table 4). Achieved results indicated that reaction yields decreased by increasing the length of the alkyl chain (compare the yield of products **18–22**, Table 4) and moving from butanal to dodecanal the reaction yield dropped from 86% (Table 4, product **20**) to 50% yield (Table 4, product **22**). Unfortunately, Zn(4)@CC did not promote the photooxidation of formaldehyde to formic acid (**19**).

When aromatic aldehydes were used as substrates, the presence of EDG substituents had a negative effect and while benzaldehyde was transformed into benzoic acid **23** in a quantitative yield, a decrease of the reaction yield was observed in the synthesis of products **24–25** (86% and 65% yield, respectively). The reaction of aldehydes functionalized with oxygen-containing groups (OMe or OH) caused the drop of the reaction yield to 36% and 30% for products **26** and **27**, respectively. Good yields were instead observed by reacting electron-poor aromatic rings, products **28** and **29** were obtained in 87% and 76% yield, respectively.

In order to test the photoactive power of Zn(4)@CC, the synthesis of **18** was performed with 0.15% and 0.075% mol of the photoactive species; The desired compounds were respectively obtained in 60% and 62% yield to prove the good activity of heterogeneous material also at very low loadings (Table 4).

## Conclusions

We here report the synthesis and complete characterization of Zn(4)@CC material that demonstrated good photoactivity in the conversion of amines into imines and aldehydes into corresponding acids. Both reactions occurred in the presence of molecular oxygen and white light and by using mild experimental conditions. The use of the Colour Catcher® support is



highly innovative for several reasons: i) low toxicity and low ecological impact of the so-obtained material; ii) economic convenience and high availability of Colour Catcher® sheets; iii) easy and efficient anchorage of the photoactive species; iv) easy recyclability of the material due to its high chemo-physical robustness and the lack of substance leaching.

Thus, data here described can be considered a valued starting point for developing further applications of this material both in catalytic reactions and sensing technologies.

## Experimental Section

General methods, characterizations and NMR spectra of isolated compounds are reported in supporting information.

**Synthesis of 1.** KOH (139.8 mg,  $2.49 \times 10^{-3}$  mol) was dissolved in 700  $\mu\text{L}$  of distilled water and added to 50.0 mL of a 10% solution of propargyl alcohol in THF, already placed in a two-necked round bottom flask. The obtained mixture was heated up to reflux and then 10.0 mL of THF solution of  $\text{F}_{20}\text{TPPH}_2$  (250.0 mg,  $2.51 \times 10^{-4}$  mol) was added dropwise. The reaction mixture was refluxed for 8 h until the complete consumption of the starting porphyrin was observed by TLC ( $\text{SiO}_2$ , *n*-hexane/ $\text{CH}_2\text{Cl}_2 = 6:4$ ). At the end of the reaction, residual KOH was quenched with HCl 1.0 N until neutral pH and then the solvent was evaporated to dryness. The obtained crude was dissolved in  $\text{CH}_2\text{Cl}_2$  (100.0 mL) and washed with water ( $3 \times 100.0$  mL). The organic phase was dried over  $\text{Na}_2\text{SO}_4$ , filtered and the solvent was evaporated to dryness. The crude was purified by flash chromatography ( $\text{SiO}_2$ , gradient elution from *n*-hexane/ $\text{CH}_2\text{Cl}_2 = 90:10$  to *n*-hexane/ $\text{CH}_2\text{Cl}_2 = 70:30$ ) to yield **1** as a purple solid (260 mg, 90% yield).  $^1\text{H}$  NMR (300 MHz, THF- $d_6$ ):  $\delta = 9.14$  (s, 8H,  $\text{H}_{\beta\text{pyrr}}$ ), 5.31 (d,  $J = 2.5$  Hz, 8H,  $\text{H}_{\text{CH}_2}$ ), 3.41 (q,  $J = 5.4$ , 3.9 Hz, 4H,  $\text{H}_{\text{CH}_3}$ ),  $-2.74$  ppm (s, 2H,  $\text{NH}_{\text{pyrr}}$ ).  $^{19}\text{F}$  NMR (376 MHz, THF- $d_6$ ):  $\delta = -140.80$  (dd,  $J = 23.8$ , 9.4 Hz),  $-157.57$  ppm (dd,  $J = 23.0$ , 8.6 Hz).  $^{13}\text{C}$  NMR (101 MHz, THF- $d_6$ ):  $\delta = 131.23$  ( $\text{C}_{\text{porph.ring}}$ ), 104.16 ( $\text{C}_{\text{porph.ring}}$ ), 78.16 ( $\text{C}_{\text{CH}_2}$ ), 62.07 ppm ( $\text{C}_{\text{CH}_2}$ ). LR-MS (ESI):  $m/z$  [ $\text{C}_{56}\text{H}_{22}\text{F}_{16}\text{N}_4\text{O}_4$ ] calcd.: 1118.14; found [ $\text{M} + \text{H}$ ] $^+$  1119.41. UV-Vis:  $\lambda_{\text{max}}$  ( $\text{CH}_2\text{Cl}_2$ )/nm (log  $\epsilon$ ): 413 (5.48), 507 (4.35), 584 (3.75). Elemental analysis calc. for [ $\text{C}_{56}\text{H}_{22}\text{F}_{16}\text{N}_4\text{O}_4$ ]: C, 60.12; H, 1.98; N, 5.01; found: C, 58.80; H, 2.43; N, 4.53.

**Synthesis of Zn(1).** Porphyrin **1** (260.0 mg,  $2.33 \times 10^{-4}$  mol) was dissolved in  $\text{CH}_2\text{Cl}_2$  (80.0 mL) and  $\text{Zn}(\text{OAc})_2 \cdot 2\text{H}_2\text{O}$  (514.0 mg,  $2.34 \times 10^{-3}$  mol) was dissolved in MeOH (20.0 mL). The zinc solution was added to the porphyrin solution and the mixture was refluxed overnight. At the end of the reaction, the solvent was evaporated to dryness and the crude was dissolved in  $\text{CH}_2\text{Cl}_2$  (150 mL) and washed with water ( $4 \times 100.0$  mL). The organic phase was dried over  $\text{Na}_2\text{SO}_4$ , filtered and the solvent was evaporated to dryness to yield **Zn(1)** as a purple solid (275.4 mg, quantitative yield).  $^1\text{H}$  NMR (400 MHz, THF- $d_6$ ):  $\delta = 9.05$  (s, 8H,  $\text{H}_{\beta\text{pyrr}}$ ), 5.30 (d,  $J = 2.4$  Hz, 8H,  $\text{H}_{\text{CH}_2}$ ), 3.40 ppm (t,  $J = 2.4$  Hz, 4H,  $\text{H}_{\text{CH}_3}$ ).  $^{19}\text{F}$  NMR (376 MHz, THF- $d_6$ ):  $\delta = -140.92$ – $-141.12$  (m),  $-158.07$ – $-158.35$  ppm (m).  $^{13}\text{C}$  NMR (101 MHz, THF- $d_6$ ):  $\delta = 150.18$  ( $\text{C}_{\text{porph.ring}}$ ), 131.42 ( $\text{C}_{\text{porph.ring}}$ ), 78.07 ( $\text{C}_{\text{CH}_2}$ ), 62.00 ppm ( $\text{C}_{\text{CH}_2}$ ). LR-MS (ESI):  $m/z$  [ $\text{C}_{56}\text{H}_{20}\text{F}_{16}\text{N}_4\text{O}_4\text{Zn}$ ] calcd.: 1181.05; found [ $\text{M} + \text{H}$ ] $^+$ : 1182.17. UV-Vis:  $\lambda_{\text{max}}$  ( $\text{CH}_2\text{Cl}_2$ )/nm (log  $\epsilon$ ): 421 (5.75), 552 (4.30), 623 (3.15). Elemental analysis calc. for [ $\text{C}_{56}\text{H}_{20}\text{F}_{16}\text{N}_4\text{O}_4\text{Zn}$ ]: C, 56.90; H, 1.71; N, 4.74; found: C, 56.69; H, 2.35; N, 4.20.

**Synthesis of Zn(3).** **Zn(1)** (275.0 mg,  $2.33 \times 10^{-4}$  mol) and methyl-3-azide-propionate (**2**) (131.0  $\mu\text{L}$ ,  $1.18 \times 10^{-3}$  mol) were dissolved in THF (55.0 mL) and thermostated at 50 °C.  $\text{CuSO}_4 \cdot 5\text{H}_2\text{O}$  (293.7 mg,  $1.18 \times 10^{-3}$  mol) was dissolved in distilled water (14.0 mL) as well as sodium ascorbate (233.1 mg,  $1.18 \times 10^{-3}$  mol). The two aqueous solutions were added to the porphyrin solution and stirred overnight at 50 °C. At the end of the reaction, the solvent was evaporated to dryness. The crude

was dissolved in  $\text{CH}_2\text{Cl}_2$  (100.0 mL) and washed with brine (100.0 mL) and water ( $3 \times 100.0$  mL). The organic phase was dried over  $\text{Na}_2\text{SO}_4$ , filtered and the solvent was evaporated to dryness. The crude was purified by flash chromatography ( $\text{SiO}_2$ , gradient elution from  $\text{CH}_2\text{Cl}_2$  to  $\text{CH}_2\text{Cl}_2/\text{MeOH} = 98:2$ ) to yield **Zn(3)** as a purple solid (244.8 mg, 62% yield).  $^1\text{H}$  NMR (400 MHz, THF- $d_6$ ):  $\delta = 9.04$  (s, 8H,  $\text{H}_{\beta\text{pyrr}}$ ), 8.24 (s, 4H,  $\text{H}_{\text{triazole}}$ ), 5.72 (s, 8H,  $\text{H}_{\text{CH}_2\text{O}}$ ), 4.80 (t,  $J = 6.6$  Hz, 8H,  $\text{H}_{\text{CH}_2\text{N}}$ ), 3.09 ppm (t,  $J = 6.6$  Hz, 8H,  $\text{H}_{\text{CH}_2\text{CO}}$ ).  $^{19}\text{F}$  NMR (282 MHz, THF- $d_6$ ):  $\delta = -141.56$ – $-141.75$  (m),  $-158.57$ – $-158.75$  (m).  $^{13}\text{C}$  NMR (101 MHz, THF- $d_6$ ):  $\delta = 150.19$  ( $\text{C}_{\text{porph.ring}}$ ), 131.48 ( $\text{C}_{\beta\text{pyrr}}$ ), 124.71 ( $\text{C}_{\text{Htriazole}}$ ), 67.67 ( $\text{C}_{\text{CH}_2\text{O}}$ ), 45.39 ( $\text{C}_{\text{CH}_2\text{N}}$ ), 33.99 ppm ( $\text{C}_{\text{CH}_2\text{CO}}$ ). LR-MS (MALDI):  $m/z$  [ $\text{C}_{72}\text{H}_{48}\text{F}_{16}\text{N}_{16}\text{O}_{12}\text{Zn}$ ] calcd.: 1696.27; found [ $\text{M} + \text{H}$ ] $^+$ : 1697.60. UV-Vis:  $\lambda_{\text{max}}$  ( $\text{CH}_2\text{Cl}_2$ )/nm (log  $\epsilon$ ): 421 (5.68), 551 (4.32). Elemental analysis calc. for [ $\text{C}_{72}\text{H}_{48}\text{F}_{16}\text{N}_{16}\text{O}_{12}\text{Zn}$ ]: C, 50.91; H, 2.85; N, 13.19; found: C, 54.89; H, 4.92; N, 9.97.

**Synthesis of Zn(4).** **Zn(3)** (128.1 mg,  $7.55 \times 10^{-5}$  mol) was dissolved in THF (30.0 mL) and EtOH (15.0 mL). An aqueous solution of KOH 2 M (20.0 mL) was added dropwise to the porphyrin solution and the mixture was stirred at room temperature overnight until the complete consumption of the starting porphyrin was observed by TLC ( $\text{SiO}_2$ ,  $\text{CH}_2\text{Cl}_2/\text{MeOH} = 95:5$ ). No other spots were observed to indicate a quantitative conversion of **Zn(3)** into **Zn(4)**. After standing for 12 h, a biphasic mixture was forming and the removal of a colorless supernatant water phase gave a solution containing **Zn(4)**. Any attempt to recover the desired product from this mixture failed. A jellyfish mixture was formed either when a apolar solvent was added to precipitate **Zn(4)** or the mixture was evaporated to dryness. Thus, the so-obtained solution was employed for the anchoring procedure without further purifications. UV-Vis:  $\lambda_{\text{max}}$  (THF/EtOH (2:1))/nm (log  $\epsilon$ ): 420 (5.21), 504 (4.02), 584 (3.71).

**Anchoring procedure for the preparation of Zn(4)@CC.** 50.0 mL of **Zn(4)**-containing solution, with the fixed concentration of  $1.50 \times 10^{-3}$  M, were placed in a coded test tube and then 92  $\text{cm}^2$  of rolled Colour Catcher® were immersed in the solution. The sheet was left in the solution for 24 h and, to prevent the porphyrin degradation, the tube was wrapped with aluminum kitchen foil. After this time, the sheet was extracted and dried on a heated plate (at 85 °C). Then it was washed with distilled water, THF and  $\text{CH}_3\text{CN}$  and dried at each step. The obtained colored sheet was finally washed with hot  $\text{CH}_3\text{CN}$  to mimic the reaction conditions. No leaching of porphyrin was observed, demonstrating an excellent adsorption of porphyrin onto the solid surface. After the last wash, the sheet was pulled out from the solvent and placed directly into a coded test tube and dried in vacuum. The obtained **Zn(4)@CC** was weighed and stored wrapped in aluminum kitchen foil. Determination of the amount of porphyrin anchored onto the Colour Catcher® was performed by UV-visible by measuring the concentration of the **Zn(4)**-containing solution before and after the immersion of the sheet. Collected data allowed estimating an average value of anchored **Zn(4)** equal to 0.24  $\text{mg}/\text{cm}^2$ .

**General procedure for the photooxidative coupling of amines.** 10.5  $\text{cm}^2$  of **Zn(4)@CC** (0.3% mol,  $1.54 \times 10^{-6}$  mol of anchored **Zn(4)**) were cut into small squares ( $\sim 10$   $\text{mm}^2$ ) and dipped into 2.5 mL of  $\text{CH}_3\text{CN}$  already placed in a 10.0 mL test tube equipped with a screw cup with a silicon/PTFE septum. Oxygen was bubbled into the mixture for 5 min and subsequently an oxygen balloon was placed on the reactor to ensure the oxygen atmosphere. The desired amine ( $5.05 \times 10^{-4}$  mol) was added to the mixture and then the white LED was switched on. The reaction was stirred at room temperature for 6 h. At the end of the reaction, **Zn(4)@CC** was filtered off and washed three times with  $\text{CH}_2\text{Cl}_2$  ( $3 \times 3.0$  mL). The organic phases were collected and dried under vacuum. The obtained crude was analyzed by  $^1\text{H}$  NMR with mesitylene as the internal standard.





**General procedure for the photooxidation of aldehydes.** 22 cm<sup>2</sup> of Zn(4)@CC (0.3% mol, 3.20 × 10<sup>-6</sup> mol of anchored Zn(4)) were cut into small squares (~10 mm<sup>2</sup>) and dipped into 5.0 mL of CH<sub>3</sub>CN already placed in a two-necked round bottom flask equipped with a condenser and a screw cup with a silicon/PTFE septum. Oxygen was bubbled into the mixture for 5 min and subsequently an oxygen balloon was placed on the reactor to ensure the oxygen atmosphere. The reactor was placed in a pre-heated water bath thermostated at 50 °C. The desired aldehyde (1.01 × 10<sup>-3</sup> mol) was added to the mixture and the halogen lamp was switched on. The reaction was carried out at 50 °C for 6 h. At the end of the reaction, Zn(4)@CC was filtered off and washed three times with CH<sub>2</sub>Cl<sub>2</sub> (3 × 5.0 mL). The organic phases were collected and dried under vacuum. The obtained crude was analyzed by <sup>1</sup>H NMR with 2,4-dinitrotoluene as the internal standard.

## Acknowledgements

C.D. R.P. and EG thanks Istituto Nazionale Assicurazione contro gli Infortuni sul Lavoro (INAIL) through the project BRIC2018-ID 05. C.D. and E.G. thank Università degli Studi di Milano for PSR 2021 – financed project "Design and synthesis of high added-value fine-chemicals by sustainable catalytic approaches" Laboratory of homogeneous Catalysis for Sustainable synthesis – LCS

## Conflict of Interests

The authors declare no conflict of interest.

## Data Availability Statement

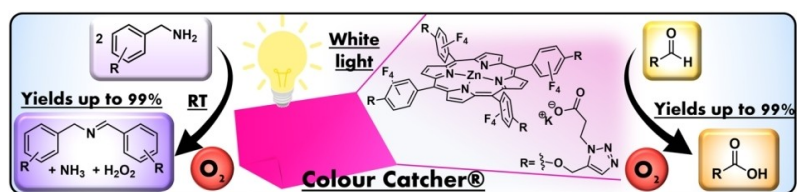
The data that support the findings of this study are available on request from the corresponding author. The data are not publicly available due to privacy or ethical restrictions.

**Keywords:** Colour Catcher · light · photocatalysis · photosensitizer · porphyrin

- [1] S. Singh, in *Energy Crisis and Climate Change*. In Energy (Eds: P. Singh, S. Singh, G. Kumar and P. Baweja). Wiley-VCH, Weinheim, Germany **2021**, pp. 1–17
- [2] N. Kannan, D. Vakeesan, *Renewable Sustainable Energy Rev.* **2016**, *62*, 1092–1105.
- [3] E. Kabir, P. Kumar, S. Kumar, A. A. Adelodun, K.-H. Kim, *Renewable Sustainable Energy Rev.* **2018**, *82*, 894–900.
- [4] M. B. Hayat, D. Ali, K. C. Monyake, L. Alagha, N. Ahmed, *Int. J. Energy Res.* **2019**, *43*, 1049–1067.
- [5] N. S. M. N. Izam, Z. Itam, W. L. Sing, A. Syamsir, *Energies* **2022**, *15*, 2790.
- [6] V. Krewald, M. Retegan, D. A. Pantazis in *Solar Energy for Fuels* (Eds.: H. Tüysüz, C. K. Chan), Springer International Publishing, Cham, **2016**, pp. 23–48.
- [7] T. P. Yoon, M. A. Ischay, J. Du, *Nat. Chem.* **2010**, *2*, 527–532.
- [8] L. Marzo, S. K. Pagire, O. Reiser, B. König, *Angew. Chem. Int. Ed.* **2018**, *57*, 10034–10072; *Angew. Chem.* **2018**, *130*, 10188–10228.
- [9] B. Zhang, L. Sun, *Chem. Soc. Rev.* **2019**, *48*, 2216–2264.
- [10] C. Spagnol, L. C. Turner, R. W. Boyle, *J. Photochem. Photobiol. B* **2015**, *150*, 11–30.
- [11] G. Obaid, M. Broekgaarden, A.-L. Bulin, H.-C. Huang, J. Kuriakose, J. Liu, T. Hasan, *Nanoscale* **2016**, *8*, 12471–12503.
- [12] H. Chen, Y. Zhao, *ACS Appl. Mater. Interfaces* **2018**, *10*, 21021–21034.
- [13] M. Ogawa, H. Takakura, *Bioorg. Med. Chem.* **2021**, *43*, 116274.
- [14] X. Li, J. Xie, C. Jiang, J. Yu, P. Zhang, *Front. Environ. Sci. Eng.* **2018**, *12*, 14.
- [15] M. B. Tahir, H. Kiran, T. Iqbal, *Environ. Sci. Pollut. Res. Int.* **2019**, *26*, 10515–10528.
- [16] X. Yang, Z. Chen, W. Zhao, C. Liu, X. Qian, M. Zhang, G. Wei, E. Khan, Y. Hau Ng, Y. Sik Ok, *Chem. Eng. J.* **2021**, *405*, 126806.
- [17] X. Lang, X. Chen, J. Zhao, *Chem. Soc. Rev.* **2014**, *43*, 473–486.
- [18] N. Corrigán, S. Shanmugam, J. Xu, C. Boyer, *Chem. Soc. Rev.* **2016**, *45*, 6165–6212.
- [19] S. G. E. Amos, M. Garreau, L. Buzzetti, J. Waser, *Beilstein J. Org. Chem.* **2020**, *16*, 1163–1187.
- [20] S. Gisbertz, B. Pieber, *ChemPhotoChem* **2020**, *4*, 456–475.
- [21] K. S. Pushpan, S. Venkatraman, G. V. Anand, J. Sankar, D. Parmeswaran, S. Ganesan, K. T. Chandrashekar, *Curr. Med. Chem. Anti-Cancer Agents* **2002**, *2*, 187–207.
- [22] L. M. Moreira, F. Vieira dos Santos, J. P. Lyon, M. Maftoum-Costa, C. Pacheco-Soares, N. Soares da Silva, *Aust. J. Chem.* **2008**, *61*, 741–754.
- [23] H. Abrahamse, M. R. Hamblin, *Biochem. J.* **2016**, *473*, 347–364.
- [24] A. Aggarwal, D. Samaroo, I. R. Jovanovic, S. Singh, M. P. Tuz, M. R. Mackiewicz, *J. Porphyrins Phthalocyanines* **2019**, *23*, 729–765.
- [25] R. Costa e Silva, L. Oliveira da Silva, A. de Andrade Bartolomeu, T. J. Brocksom, K. T. de Oliveira, *Beilstein J. Org. Chem.* **2020**, *16*, 917–955.
- [26] N. End, K.-U. Schöning in *Immobilized Catalysts: Solid Phases, Immobilization and Applications* (Ed.: A. Kirschning), Springer Berlin Heidelberg, Berlin, Heidelberg, **2004**, pp. 241–271.
- [27] A. E. C. Collis, I. T. Horváth, *Catal. Sci. Technol.* **2011**, *1*, 912–919.
- [28] O. Piematti, R. Abu-Reziq, L. Vaccaro in *Catalyst Immobilization*, **2020**, pp. 1–22.
- [29] C. H. Mak, X. Han, M. Du, J.-J. Kai, K. F. Tsang, G. Jia, K.-C. Cheng, H.-H. Shen, H.-Y. Hsu, *J. Mater. Chem. A* **2021**, *9*, 4454–4504.
- [30] F. Caroleo, G. Magna, C. Damiano, M. Cavalleri, E. Gallo, C. Di Natale, R. Paolesse, *Sens. Actuators B* **2022**, *364*, 131900.
- [31] M. Luoni, G. Li Bassi, "Non-woven Colour-Catcher fabric and method for its preparation" (U.S. Patent No. US2009/0137170 A1), **2009**; P. McNamee, K. Schmitz, E. Guilmet, "Dye catching laundry sheet", World Intellectual Property Organization, (Patent No.: WO2017118630 A1) **2017**.
- [32] Y.-Y. Huang, T. Balasubramanian, E. Yang, D. Luo, J. R. Diers, D. F. Bocian, J. S. Lindsey, D. Holten, M. R. Hamblin, *ChemMedChem* **2012**, *7*, 2155–2167.
- [33] J. M. Dąbrowski, B. Pucelik, M. M. Pereira, L. G. Arnaut, G. Stochel, *J. Coord. Chem.* **2015**, *68*, 3116–3134.
- [34] L. De Boni, C. J. P. Monteiro, C. R. Mendonça, S. C. Zilio, P. J. Gonçalves, *Chem. Phys. Lett.* **2015**, *633*, 146–151.
- [35] H.-G. Jeong, M.-S. Choi, *Isr. J. Chem.* **2016**, *56*, 110–118.
- [36] C. Damiano, S. Gadolini, D. Intriari, L. Lay, C. Colombo, E. Gallo, *Eur. J. Inorg. Chem.* **2019**, *41*, 4412–4420.
- [37] K. Ladomenou, V. Nikolaou, G. Charalambidis, A. G. Coutsolelos, *Coord. Chem. Rev.* **2016**, *306*, 1–42.
- [38] M. Bregnhøj, M. Westberg, F. Jensen, P. R. Ogilby, *Phys. Chem. Chem. Phys.* **2016**, *18*, 22946–22961.
- [39] J. A. Johnson, J. Luo, X. Zhang, Y.-S. Chen, M. D. Morton, E. Echeverria, F. E. Torres, J. Zhang, *ACS Catal.* **2015**, *5*, 5283–5291.
- [40] L. Huang, J. Zhao, S. Guo, C. Zhang, J. Ma, *J. Org. Chem.* **2013**, *78*, 5627–5637.
- [41] X. Yang, T. Huang, S. Gao, R. Cao, *J. Catal.* **2019**, *378*, 248–255.
- [42] C. Liu, K. Liu, C. Wang, H. Liu, H. Wang, H. Su, X. Li, B. Chen, J. Jiang, *Nat. Commun.* **2020**, *11*, 1047.
- [43] A. Sanches-Silva, A. R. de Quirós, J. López-Hernández, P. Paseiro-Losada, *J. Chromatogr. A* **2004**, *1046*, 75–81.
- [44] U. R. A. Svedberg, H.-E. Högberg, J. Högberg, B. Galle, *Ann. Occup. Hyg.* **2004**, *48*, 339–349.
- [45] L. Ernstgård, A. Iregren, B. Sjögren, U. Svedberg, G. Johanson, *J. Occup. Environ. Med.* **2006**, *48*, 573–580.
- [46] M. Corradi, I. Rubinstein, R. Andreoli, P. Manini, A. Caglieri, D. Poli, R. Alinovi, A. Mutti, *Am. J. Respir. Crit. Care Med.* **2003**, *167*, 1380–1386.
- [47] P. Fuchs, C. Loeseken, J. K. Schubert, W. Miekisch, *Int. J. Cancer* **2010**, *126*, 2663–2670.

Version of record online: May 5, 2023

## RESEARCH ARTICLE



The anchorage of zinc(II) porphyrin onto Colour Catcher® sheets allows obtaining a powerful photoactive material able to promote oxidative reactions in the presence of pure molecular oxygen and white light. The

good performance and chemophysical stability of the Colour Catcher®-based material pave the way for its employment in eco-friendly photochemical processes.

Dr. C. Damiano, M. Cavalleri, Prof. C. di Natale\*, Prof. R. Paolesse, Prof. E. Gallo\*

1 – 10

**Porphyrins Anchored onto Colour Catcher®: Photoactive Material for the Conversion of Amines into Imines and Aldehydes into Carboxylic Acids**

